Pediatric Cardiology
https://doi.org/10.1007/s00246-021-02790-z

ORIGINAL ARTICLE

# Deep Learning-Based Approach to Automatically Assess Coronary Distensibility Following Kawasaki Disease

Mitchel Benovoy[1,2] · Audrey Dionne[1,3] · Brian W. McCrindle[4] · Cedric Manlhiot[4] · Ragui Ibrahim[5] · Nagib Dahdah[1]

Received: 27 July 2021 / Accepted: 20 November 2021


## Abstract

Kawasaki disease is an acute vasculitis affecting children, which can lead to coronary artery (CA) aneurysms. Optical coherence tomography (OCT) has identified CA wall damage in KD patients, but it is unclear if these findings correlate with any distensibility changes in the CA and how these changes evolve over time. This paper seeks to establish the link between OCT findings and vessel distensibility with a novel deep learning coronary artery segmentation system and use the segmentation framework to automatically analyze the temporal evolution of coronary stiffness over many years. 27 KD patients underwent catheterization with coronary angiography of the left coronary artery (LCA), followed by OCT of proximal and distal segments of the LCA. Changes in the CA caliber over the cardiac cycle were measured automatically and compared against OCT findings suggestive of KD-related vascular damage. In addition, 34 KD patients with regressed or persistent CA aneurysms were followed with serial CA angiography over an average of 14.5 years. Distensibility changes were calculated using a deep learning coronary artery segmentation framework and evaluated longitudinally. Distensibility in the coronary arteries after KD negatively correlated with increasing severity of OCT findings of KD-related vessel damage. KD patients have a significant increase in CA wall stiffness at 1 year after diagnosis, which then plateaus subsequently, compared to controls. Also, patients with persistent CA aneurysms have a statistically significant increase in wall stiffness over time in comparison to those with regressed CA aneurysms. Distensibility changes in the CA of KD patients calculated using our automated deep learning approach correlates with the severity of OCT findings of KD-related CA damage. This decreased distensibility peaks at 1 year in KD patients when following longitudinally and is more severe in those with persistent CA aneurysms.

**Keywords** OCT · Kawasaki · Aneurysm · Distensibility · Coronary artery

## Introduction

Kawasaki disease (KD) is an acute febrile vasculitis of unknown etiology that affects the medium-sized arteries. KD especially targets the coronary arteries, and a common serious complication in untreated cases is the development of coronary artery aneurysms, which may lead to sudden death [1]. The involved arteries show an acute inflammatory infiltrate (neutrophils, $CD8^+$ T cells, dendritic cells) which leads to fragmentation of the internal elastic laminae and vascular damage [2]. Prompt diagnosis and treatment of KD is critical for preventing the formation of coronary artery aneurysms (CAA). Treatment with intravenous immunoglobulin (IVIG) in the acute phase can decrease the risk of developing CAA from 25% to less than 5% [3]. Echocardiography is used for the diagnosis and follow-up of CAA. However, patients with coronary artery complications may require further imaging [3].

✉ Nagib Dahdah
nagib.dahdah.hsj@ssss.gouv.qc.ca

1 Division of Pediatric Cardiology, CHU Ste-Justine, University of Montreal, 3175, Côte Sainte-Catherine, Montreal, QC H3T 1C5, Canada

2 Circle Cardiovascular Imaging Inc., Montreal, QC, Canada

3 Division of Pediatric Cardiology, Department of Pediatrics, Boston Children's Hospital, Harvard Medical School, Boston, MA, USA

4 Department of Pediatrics, University of Toronto, Labatt Family Heart Centre, The Hospital for Sick Children, Toronto, ON M5G 1X8, Canada

5 Division of Cardiology, Pierre Boucher Hospital, Longueuil, QC, Canada

Published online: 02 December 2021

Although current conventional cardiac imaging techniques, which include echocardiography, cardiac computed tomography (CT), magnetic resonance imaging (MRI) angiography, and invasive x-ray angiography, can provide information on aneurysm size, location, and concomitant stenosis, they are of limited use in providing detailed information about coronary vessel wall components. Optical coherence tomography is a light-based imaging modality that generates high-resolution cross-sectional images of tissue microstructures. It provides nearly 10 times higher axial resolutions compared to intravascular ultrasound (IVUS) and a spatial resolution of up to 12–15 μm [4]. Hence, information such as the presence of intimal hyperplasia, neovascularization, microcalcifications, and other vessel irregularities can be seen both in coronary artery aneurysms and nearby adjacent normal appearing regions [5–7] and has been used to precisely characterize sequalae in KD [8, 9].

Although anatomical changes in coronary arteries occur as part of the sequelae of KD, it is also known that decreased vessel wall distensibility correlates with vascular dysfunction. Our group has developed a novel angiography-based system to assess vascular wall motion with automatic vessel segmentation and spatiotemporal vessel tracking. This efficient method allows for the analysis of longitudinal data on the vessel caliber across the cardiac cycle, which permits calculation of metrics related to coronary artery distensibility. The purpose of this study was (1) to ascertain whether reduced distensibility (increased stiffness) correlates with OCT findings, and (2) to evaluate the distensibility changes longitudinally over time in patients with and without CAA.

## Methods

### Overview and Subjects

Children diagnosed with KD based on clinical criteria with or without history of CAA were included in this study. In the first part of the study, we evaluated CA distensibility in a series of KD patients and comparatively validated these changes against OCT findings of KD-related vessel damage [10]. In the second part of this study, we evaluated and compared CA distensibility evolution longitudinally in 3 subject groups: normal controls (CTL), KD patients with regressed CA aneurysms (KDREG), and KD patients with persistent CA aneurysms (KDPER). CA angiography was obtained for suspected symptoms in some cases and by standard clinical practice in others. OCT analysis of both proximal and distal segments of the left coronary artery (LCA) was performed at time of cardiac catheterization. Data were collected at a single time point for all subjects. OCT interpretation was performed by an operator blinded to CA aneurysmal status. Controls were patients who had undergone selective coronary angiography for a reason unrelated to Kawasaki disease and had intact coronary arteries (i.e., no history of known inflammatory, congenital, acquired disease or surgery to affect the coronary arteries). This retrospective study was approved by participating ethics review boards. Parental consent was obtained for OCT imaging.

### Data Definition

Echocardiogram-based Z-scores of aneurysms from serial follow-up were used to classify KD patients into the KDREG or KDPER groups. Regressed aneurysm was defined as a coronary $Z$-score $< 2$ on echocardiogram at the time of angiography and OCT. Coronary angiographies were performed as clinically required, either for routine follow-up or due to symptoms related to ischemia.

### Automatic CA Segmentation and Calculation of Caliber

#### Training and Testing Data

The ground truth database of 100 pediatric X-ray angiograms were used as training data. None of these patients were included in distensibility analysis cohort. For each series, the peak vessel enhancement image was isolated and used for manual annotation. To facilitate the annotation for vessel segmentation, a graphical interface was implemented to allow vector drawing of vessels as well as free drawing. To reduce annotation time, we used segmentation maps from a neural network trained to segment retina vessels. The database of 100 series was divided into two sets: 30 series for the test set and 70 series for the training set. Among these 70 series, ten were kept for validation of the segmentation system. It is on this set of ten images that the parameters of the model were optimized. The images were cropped in a patch around a central pixel labeled as an artery or as a background. The segmentation performance of the network evaluated on the test set produced an overlap measure (DICE score) of $94\% \pm 2.4\%$ compared to manual ground truth segmentation.

#### Learning Model

For reproducibility purposes, details of the neural network architecture are given here. The model used was an encoder–decoder type comprised of five layers of encoding and five layers of decoding. Each encoding layer has three convolution layers followed by a max-pooling layer. Each decoding layer has a scaling layer followed by a convolutional layer. Following the U-Net model [11], the characteristic images of the encoding section are concatenated with the characteristic images of the decoding part, thus

multiplying the number of images by two to facilitate the transfer of high-resolution characteristics. Each encoding layer reduces the size of the image by a factor of two while multiplying the number of characteristic images by four. The decoding layers reduce the number of characteristic images by a factor of two. Finally, the last convolutional layer transforms the characteristic images into an image of two channels, each channel representing the probability map of being a vessel or the background.

### Learning Strategy

The parameters of the model (weight and bias for each neuron) are initialized according to Xavier's method [12]. The training patches are sent to the input of the model and the parameters of each neuron were evolved by Adam stochastic gradient descent [13]. Finally, a realistic data augmentation strategy was used. This strategy is a key element for convolutional neural networks, especially when data are limited. The goal was to alter the input patches to increase the variability and thus obtain a model that generalizes to different patients better. The data increase was carried out by randomly adding the three main eigenvectors to the patch intensities. These eigenvectors were obtained after analysis as the main component of the patch training base.

### Optimization

The model inference code was optimized with GPU parallelization techniques to speed up the execution of vascular tree analysis tools: the skeletonization of segmentation by the Zhang-Suen algorithm [14], the calculation of the diameter by distance transform [15], and the related component setting by the Equivalence algorithm [16].

The coronary artery tree for each subject was automatically segmented (see Fig. 1) for each image/time point $t\epsilon[0, T]$ across 1–2 QRS-QRS intervals/cardiac cycles (see Fig. 2). CA centerlines were then automatically extracted, and vessel calibers were computed across the arterial tree.

## Calculation of Distensibility Metrics

For each subject, the Caliber Standard Deviation (CSD) was computed as the temporal variation of the mean of the coronary artery caliber, $C(t)$, during the time interval, $t\epsilon[0, T]$ :

$$\mathrm{CSD} = \mathrm{SD}(C(t)).$$

Two metrics of coronary artery distensibility (CA relaxation) were calculated using the caliber data: the mean constriction velocity, MCV, and the mean expansion (recoil) velocity, MEV. The two metrics are defined along the time interval, $t\epsilon[0, T]$, as follows:

$$\mathrm{MCV} = \frac{dC(t)}{dt} < 0,$$

$$\mathrm{MEV} = \frac{dC(t)}{dt} > 0.$$

Two elastic moduli were calculated for each subject from the above metrics of coronary artery distensibility and the subject's trans-myocardial blood pressure gradients, mean and pulse blood pressure readings. An elastic modulus is a measure of the stiffness of tissue and is generally defined

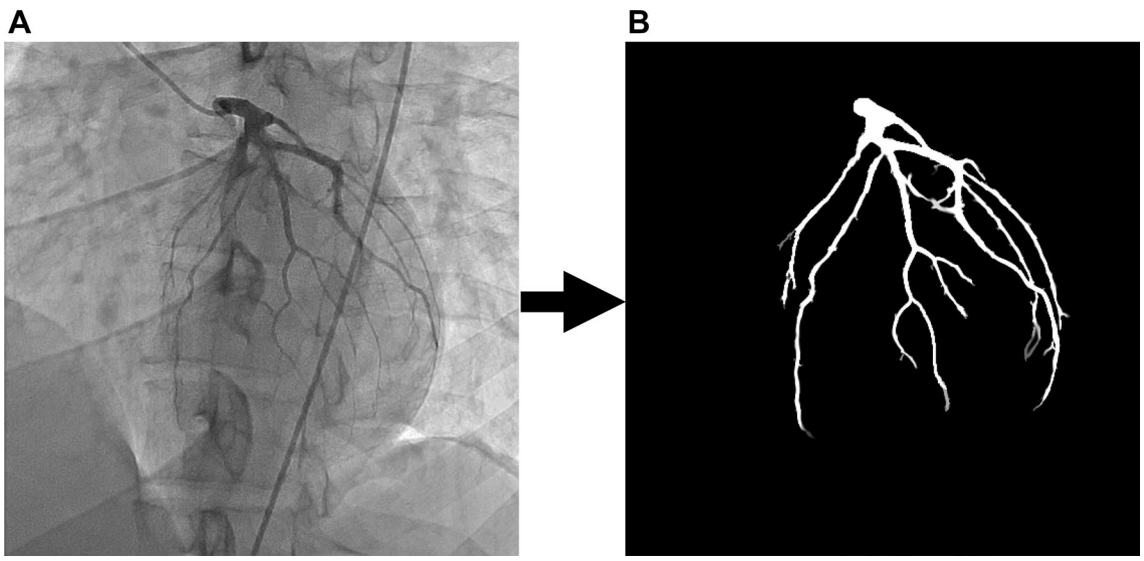


**Fig. 1** **A** Conventional angiography image showing the coronary vasculature after dye is injected into the main coronary artery. **B** Mask image showing automatic segmentation result of the coronary vasculature from the angiography data

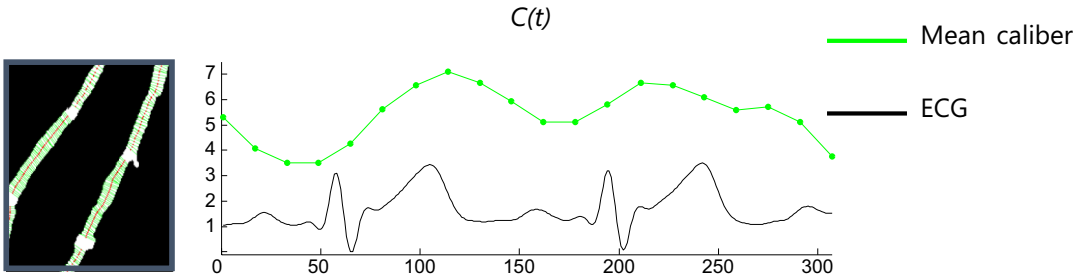


**Fig. 2** Schematic demonstrating the automated segmentation and measurement of coronary artery vessel caliber through the cardiac cycle (ECG QRS to QRS interval—black line), which is used to compute the mean vessel caliber along the segment at each time point (green line), giving the temporal profile of vessel caliber, *C(t)*

as the ratio of stress to strain, where stress is the force that produces the strain (blood pressure) and the strain is the ratio of the change in some physical parameter due to the stress to the original value of that parameter (vessel caliber). The mean pressure modulus, $CSD_{MPM}$ and the pulse pressure modulus, $CSD_{PPM}$, are defined, respectively, as follows:

$$CSD_{MPM} = \frac{\bar{BP} - LVEDP}{CSD},$$

$$CSD_{PPM} = \frac{\bar{PP} - LVEDP}{CSD},$$

where LVEDP left ventricular end diastolic pressure, CSD coronary artery caliber, $\bar{BP}$ mean blood pressure, $\bar{PP}$ pulse pressure.

## OCT Procedure and Scoring

For each subject in the validation study, OCT was performed in the proximal and distal left coronary artery (LCA) segments while undergoing cardiac catheterization, in addition to conventional angiography, as previously described by our group [5]. A Dragonfly catheter (St-Jude Medical, St Paul, MN) was advanced through a guiding coronary catheter (6 Fr or 5 Fr) following intracoronary administration of nitroglycerin. Images were analyzed offline measuring the thickest intima and thinnest media, as identified throughout the pullback. When disappearance/destruction of the media was observed, a value of 10 μm was assumed (maximal spatial resolution of OCT imaging) to allow calculation of the intima/media ratio. The images were also qualitatively analyzed for the presence of fibrosis (homogeneous high backscattering areas), and calcifications (well-demarcated borders with heterogeneous signal loss) following the consensus standards for acquisition, measurement, and reporting of OCT studies [3]. For each study segment, a numerical OCT score (from 0 to 4) was assigned based on the presence of the following specific findings (one point each): (1) intimal hyperplasia, (2) medial destruction, (3) fibrosis, (4) calcifications.

## Statistics

Kruskal–Wallis non-parametric significance tests were performed in Matlab (Natick, USA). A $P$-value $< 0.05$ was considered statistically significant. For each plot of the OCT score against a distensibility metric (represented by $x$ and $y$, respectively), the correlation coefficient ($r$) was calculated, as follows:

$$r = \frac{\sum (x - \bar{x})(y - \bar{y})}{\sqrt{\sum (x - \bar{x})^2 \sum (y - \bar{y})^2}}.$$

# Results

OCT images were collected from 27 pediatric patients diagnosed with KD based on clinical criteria who had coronary artery segments with or without history of aneurysm (Table 1). The mean age of the subjects at the time of evaluation was $12.4 \pm 5.5$ years of age. Patients' characteristics of the longitudinal distensibility analysis are summarized in Table 2, where the mean age of patients at diagnosis was $4.6 \pm 4.12$ years.

## OTC Validation of Angiography-Based Distensibility Assessment

For each subject, the calculated distensibility metrics, CSD, MEV, and MCV, were plotted against increasing severity of OCT findings (see Fig. 3). Patient with OCT evidence of more serious KD-related vessel damage had a statistically significant reduction in distensibility compared to those with little to no OTC evidence of damage. Similarly, by plotting the high-pressure moduli, $CSD_{MPM}$ and $CSD_{PPM}$, derived

**Table 1** Patients' characteristics of cases that underwent OCT imaging

| | Mean ± SD | Median [range] (proportion) |
|---|---|---|
| Male/female | | 17/10 |
| Day of fever at diagnosis (day) | 10.0 ± 4.7 | 10 [421] |
| Age at diagnosis (year) | 3.4 ± 3.4 | 3 [0.2–13.5] |
| Diagnostic criteria | | 5 [3–6] |
| Incomplete/complete criteria | | 10/17 |
| Delay to IVIG | | 9/27 (33%) |
| IVIG resistance | | 9/27 (33%) |
| WBC | 17.9 ± 5.3 | |
| Neutrophil counts (%) | 65 ± 20 | |
| Hemoglobin | 99.5 ± 12.5 | |
| Peak platelet count | 686.4 ± 294.9 | |
| CRP | 162.4 ± 94.8 | |
| Albumin | 22.4 ± 5.0 | |
| ALT | 41.8 ± 38.8 | |
| AST | 38.1 ± 21.8 | |
| Follow-up CA lesions | | |
| RCA aneurysm | | 13/18 |
| LCA aneurysm | | 14/18 |
| CX aneurysm | | 12/18 |
| Giant aneurysm | | 8/18 |
| Age at OCT imaging (year) | 12.4 ± 5.4 | 12.5 [3.5–22.2] |
| Weight at OCT (kg) | 49.9 ± 26.0 | 47.6 [17–125] |
| Height at OCT (cm) | 148.5 ± 23.0 | 152 [102–189] |
| BSA at OCT ($m^2$) | 1.41 ± 0.46 | 1.42 [0.7–2.4] |
| Intracoronary Nitroglycerin | | |
| Into RCA (mcg) | 117.1 ± 52.4 | 80.2 [31.5–208.0] |
| Into LCA (mcg) | 144.2 ± 60.5 | 150 [25–250] |

from the calculated distensibility and trans-myocardial blood pressure gradients, against increasing OTC score showed that patients with more severe evidence of KD-related CA damage had statistically significant increases in wall stiffness (Fig. 4).

## Longitudinal Angiography-Based Distensibility Assessment

We analyzed left and right CA segments from 99 angiograms performed in 5 controls (CTL) and 34 KD patients (18 KDREG, 16 KDPER) over a mean follow-up of 14.5 years. For the control patients (mean age at time of imaging = 5.7 ± 4.9 years, 4 males), 3 had non-obstructive, non-fistulous right coronary artery anatomy indicating normal anatomy and circulation, 1 had a ventricular septal defect and double chamber right-ventricle anatomy, and one adolescent had undergone an arterial switch operation at birth but presented with normal CA anatomy as imaged by angiography. CSD, a metric of vessel distensibility, was calculated for each subject and was plotted versus time for each of the 3 groups to show the temporal profile of these distensibility changes (Fig. 5). Distensibility showed a sharp decrease at one-year follow-up in both patient groups, which then plateaued for subsequent assessments.

Finally, the mean CSD, CSD, for each group was calculated from the group subjects across all time points (presented here as CSD= mean ± SD in normalized pixels (npx)) (Fig. 6). Patients in the KDREG group were associated with higher CA distensibility versus patients in the KDPER group (CSD= 0.289 ± 0.0170 npx vs. CSD= 0.240 ± 0.0199 npx, respectively, $P < 0.05$), and both groups showed increased stiffness compared to patients in the control group, CTL (CSD= 0.380 ± 0.07 npx, $P < 0.001$).

## Discussion

Patient with CAA after KD showed increased vascular stiffness and more abnormal vascular motion versus those without coronary involvement. The reduced distensibility was more marked in segments with persistent CAA than those with regressed CAA. Moreover, the OCT score, which was based on the presence of OCT findings suggestive of

**Table 2** Patients' characteristics of the longitudinal distensibility analysis

| | Mean ± SD | Median [range] (proportion) |
|---|---|---|
| Male/female | | 28/8 |
| Day of fever at diagnosis (days) | 12.4 ± 13.2 | 10 [1–78] |
| Age at diagnosis (years) | 4.5 ± 4.2[a] | 3.4 [0.2–13.5] |
| Diagnostic criteria | | 5 [2–6] |
| Incomplete/complete criteria | | 14/21 |
| Delay to IVIG | | 14/33 (42%) |
| IVIG resistance | | 13/29 (33%)[b] |
| WBC | 14.1 ± 6.4 | |
| Neutrophil counts (%) | 11.3 ± 5.6 | |
| Hemoglobin | 109.1 ± 19.4 | |
| Peak platelet count | 539.3 ± 261.4 | |
| CRP | 80.0 ± 64.1[c] | |
| Albumin | 30.5 ± 7.5 | |
| ALT | 61.3 ± 78.4 | |
| AST | 63.9 ± 65.2 | |
| Maximum *Z*-score of persistent CAA | 34.4 ± 14.0 | 33.3 [13.8–68.5] |
| Maximum *Z*-score of regressed CAA | 20.9 ± 6.8 | 20.1 [7.9–31.7][d] |
| Age at first angiography (years) | 5.87 ± 5.29 | |
| Diagnosis to first angiography (years) | 2.1 ± 4.1 | 0.3 [0–15.7] |
| First to last angiography (years) | 4.12 ± 3.5 | 2.8 [0.9–14.5] |

[a]Patients with persistent aneurysms were older (5.7 ± 4.3) at diagnosis of KD compared to those with regressed aneurysms (3.0 ± 3.9) ($P = 0.042$)

[b]Only 29/36 patients received IVIG at the time of diagnosis

[c]Higher CRP in persistent (122.2 ± 69.2) versus regressed (44.6 ± 36.2) aneurysms ($P = 0.01$)

[d]$P$ value = 0.002, comparative between persistent and regressed CAA

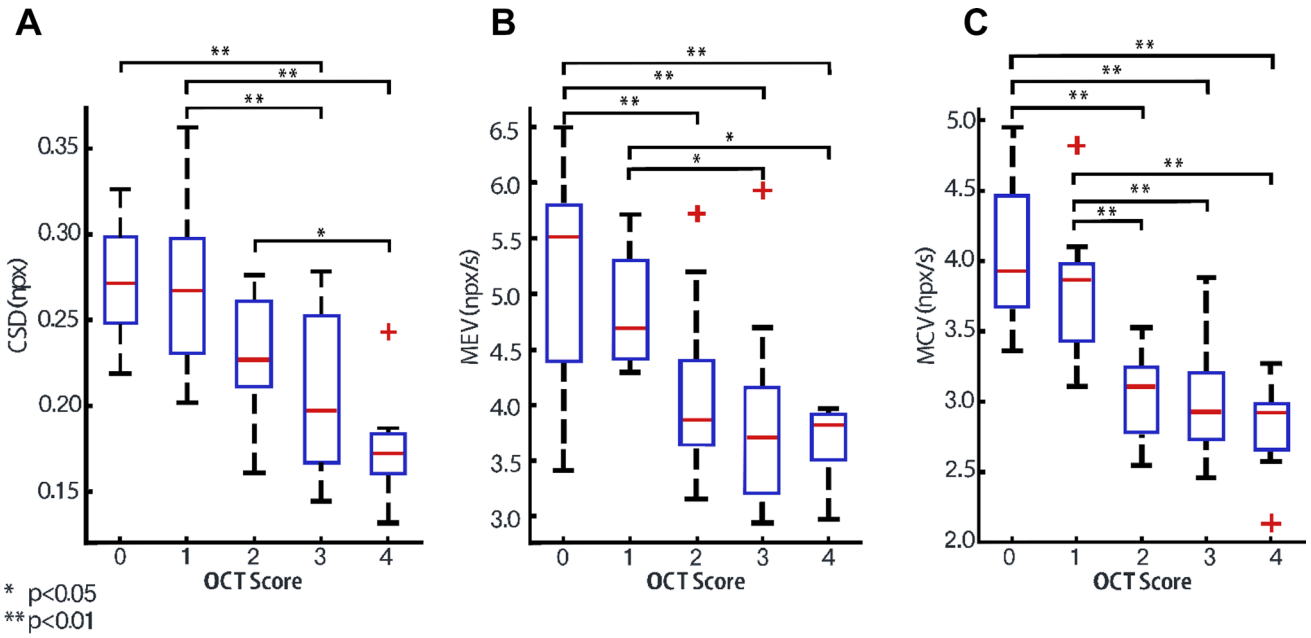


**Fig. 3** Graph of the different vessel distensibility metrics (y-axis) of the LCA segments against the increasing OTC score (x-axis) (0—normal findings to 4—signs of severe KD-related LCA damage) **A** CSD, temporal variation in the caliber of the LCA; **B** MEV, the mean expansion velocity; **C** MCV, the mean constriction velocity. Note that increasing OCT score indicating more severe vessel damage correlates with less vessel distensibility

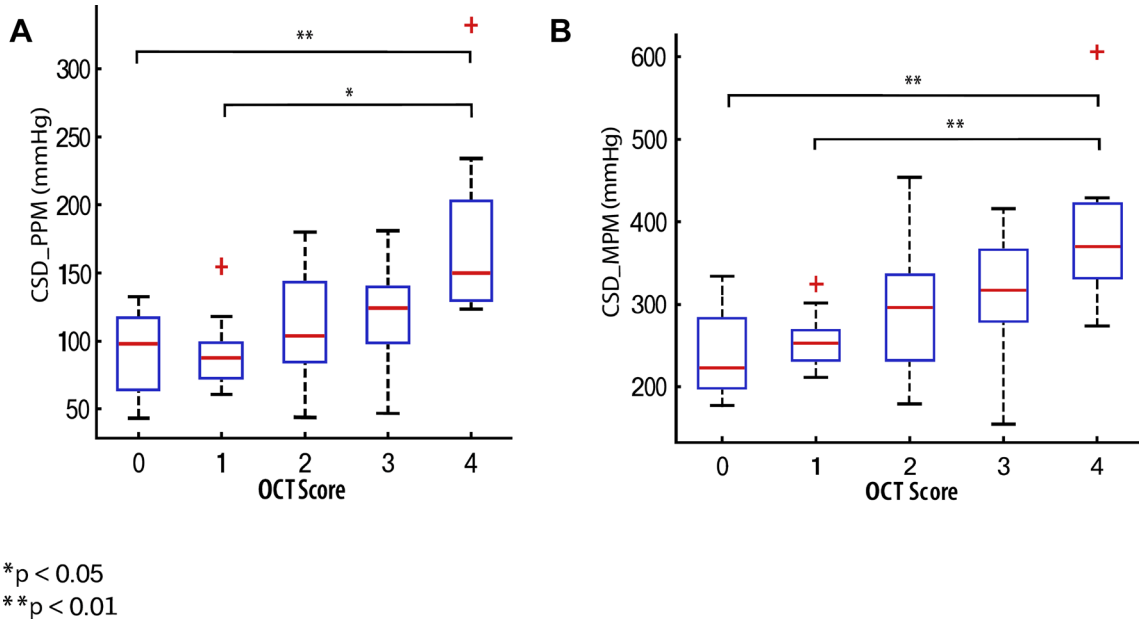


**Fig. 4** Graph of the two elastic moduli of the LCA segments (y-axis) plotted against increasing OTC score (x-axis) (0—normal findings to 4—signs of severe KD-related LCA damage) **A** Pulse pressure modulus, $CSD_{PPM}$; **B** Mean pressure modulus, $CSD_{MPM}$. Note that increasing OCT score, indicating more severe vessel damage, correlates with markedly increased wall stiffness as reflected by higher pressure-dependent moduli

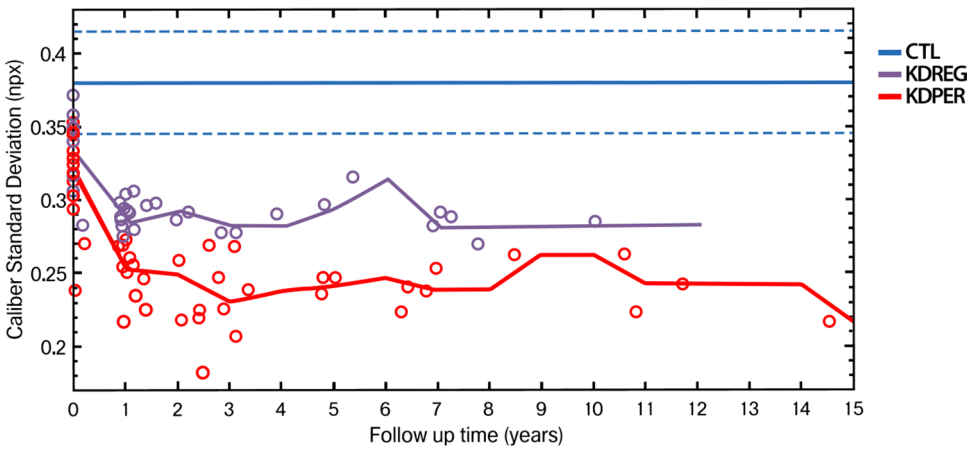


**Fig. 5** Graph showing the longitudinal effect of CSD, the temporal variation of the vessel caliber, from segments of the left and right CAs obtained from multiple CA angiograms in three different subject groups over a mean follow-up period of 14.5 years. A CTL (blue line): healthy control subjects ($n=5$), showing no change in distensibility over time. B KDREG (blue line): KD patients ($n=18$) with regressed CA aneurysm. C KDPER (red line): KD patients ($n=16$) with persistent CA aneurysms. Note the sharp decrease in distensibility at one-year follow-up followed by a plateau at subsequent assessments

KD-related vessel damage (intimal hyperplasia, calcifications, or media destruction), was positively correlated with stiffness of the vessel. Specifically, patients with OCT scores > 2 exhibited markedly increased wall stiffness and higher pressure-dependent moduli. These findings represent a bridge of knowledge between coronary parietal changes based on OCT imaging and angiography-based analysis of distensibility.

Our findings of reduced distensibility in coronary artery segments with CAA are consistent with previous reports using intracoronary acetylcholine challenges of the coronary arteries long after KD patients had sustained aneurysmal changes. Coronary artery sites of aneurysmal changes, whether regressed or persistent, exhibited reduced dilatation, and even vasoconstriction in some cases as opposed to the expected dilatation in healthy unaffected segments

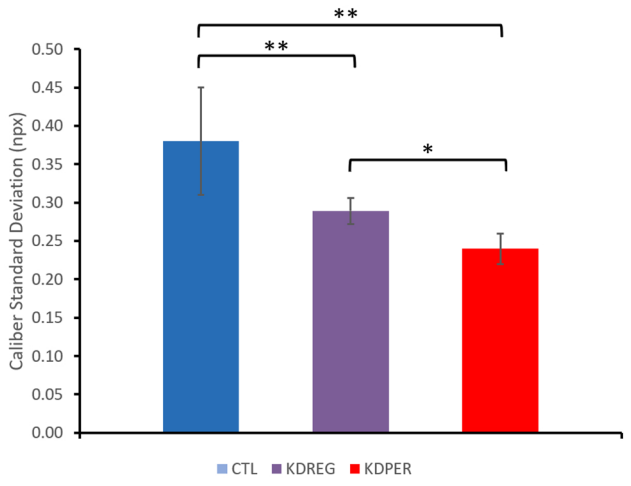


**Fig. 6** Comparison of mean CSD, $\overline{CSD}$, over the follow-up period between the three subject groups. CTL: normal healthy control group; KDREG: KD patients with regressed CA aneurysm; KDPER: KD patients with persistent CA aneurysms. KDREG was associated with higher distensibility versus KDPER ($\overline{CSD}$= 0.289 ± 0.0170 npx vs. $\overline{CSD}$= 0.240 ± 0.0199 npx, $p < 0.05$), and both groups showed increased stiffness compared to CTL ($\overline{CSD}$= 0.380 ± 0.07 npx, $p < 0.001$) [for $\overline{CSD}$ presented as mean ± SD normalized pixels (npx)]

or non KD patients [16]. Similarly, in another study using intra-coronary ultrasound, smooth muscle fibers from coronary arteries with regressed aneurysm responded poorly to nitroglycerin injection [17]. Future studies should evaluate the impact of distensibility on cardiac outcome following KD, as abnormal arterial distensibility was associated with increased risk of cardiovascular events and mortality in adults [18, 19].

The mechanism of altered CA recoil and expansion following KD remains unclear. In a previous work on OCT in KD patients, we identified a number of abnormal findings in segments with CAA: intimal hyperplasia, disappearance of the media, fibrosis, calcification, cellular infiltrates, neovascularization, and white thrombi [6, 7]. The pathological score of scar tissue grading we used in this study was based on those previously described findings. Segments with microstructural changes observed on OCT had increased vascular stiffness. Moreover, the extent of microstructural anomalies found correlated with the severity of vascular stiffness. Similarly, intra-coronary ultrasound found significantly thickened intima-media complex at sites of persistent and regressed aneurysm after KD and abnormal response to nitroglycerine in segments with history of CAA [17]. A better understanding of the underlying microstructural changes and functional impact on vascular stiffness may help improve the risk stratification of patients beyond current findings on invasive and non-invasive imaging which includes aneurysm size, stenosis, and thrombus.

Selective coronary angiography has largely been replaced by non-invasive imaging in the care of KD-related coronary complications. Echocardiography is particularly useful for the proximal segments of the coronary arteries [3], while magnetic resonance imaging (MRI) and computed tomography (CT) can assess both proximal and distal coronary segments. Fractional flow reserve is a useful tool to assess the hemodynamic significant of coronary artery lesions but has been until recently limited to invasive methods that require the insertion of a pressure wire into the coronary arteries [20, 21]. In this series, we described a new semi-automated method to assess vascular wall motion and calculate distensibility metrics using invasive angiography. An advantage of this technique is that it can be performed using the coronary angiography images and does not require the use of a pressure wire, limiting the risk of complication [22]. Moreover, future studies should validate the use of this method on coronary angiography obtained using cardiac CT [23].

This work should be interpreted in light of its limitations. The prognostic value of microvascular changes on OCT and vascular stiffness could not be assessed due to the retrospective design of the study and small patient size. In addition, OCT was only performed in the left coronary artery of KD patients, whereas the longitudinal analysis included both left and right coronary branches. This was performed because, compared to the right branch, the left coronaries typically have larger vessel calibers to accommodate the OCT probe. However, this has limited impact in the obtained results as all patients in our cohort with RCA aneurysms also had LCA aneurysms and all non-aneurysmal LCA patients also had non-aneurysmal RCA segments. The only left/right CAA imbalances were found in some patients with only LCA aneurysms, which is inconsequential as these were the OCT-imaged segments by design. Lastly, we could not study the evolution of vessel distensibility in the healthy control group to compare the known natural changes in stiffness to those in our longitudinal patient cohort.

## Conclusion

In this series, we described a new angiography-based method to assess vascular wall motion of the coronary arteries and assess metrics of coronary artery distensibility. In this proof of concept, the coronary artery segments with CAA after KD had decreased distensibility compared to segment with regressed aneurysms followed by unaffected segments. The decrease in distensibility peaked one year following KD diagnosis and persisted throughout follow-up. Moreover, distensibility changes in KD patients correlated with the severity of OCT findings in corresponding CA segments, giving insight into the pathophysiology of functional changes after KD. Future studies should focus

on the applicability of automated distensibility analysis to prospectively stratified patients with KD, and other types of vascular disease, at risk of major adverse cardiac events.

**Acknowledgements** The BoBeau Coeur Foundation provided financial support.

## Declarations

**Conflict of interest** No conflicts of interest to declare.

**Ethical Approval** This work was approved by the Ethics Institutional Board.

## References


1. Newburger JW, Takahashi M, Burns JC (2016) Kawasaki disease. J Am Coll Cardiol 67(14):1738–1749. https://doi.org/10.1016/j.jacc.2015.12.073
2. Rowley AH, Shulman ST (2010) Pathogenesis and management of Kawasaki disease. Expert Rev Anti Infect Ther 8(2):197–203. https://doi.org/10.1586/eri.09.109
3. McCrindle BW, Rowley AH, Newburger JW et al (2017) Diagnosis, treatment, and long-term management of Kawasaki disease: a scientific statement for health professionals from the American Heart Association. Circulation 135:2747
4. Tearney GJ, Regar E, Akasaka T et al (2012) Consensus standards for acquisition, measurement, and reporting of intravascular optical coherence tomography studies: a report from the International Working Group for Intravascular Optical Coherence Tomography Standardization and Validation. J Am Coll Cardiol 59(12):1058–1072. https://doi.org/10.1016/j.jacc.2011.09.079
5. Manouzi A, De Souza A, Potts JE et al (2014) Feasibility of optical coherence tomography in children with Kawasaki disease and pediatric heart transplant recipients. Circ Cardiovasc Imaging 7(4):671–678. https://doi.org/10.1161/circimaging.113.001764
6. Dionne A, Ibrahim R, Gebhard C et al (2015) Coronary wall structural changes in patients with Kawasaki disease: new insights from optical coherence tomography (OCT). J Am Heart Assoc 4(5):1–9. https://doi.org/10.1161/JAHA.115.001939
7. Dionne A, Ibrahim R, Gebhard C et al (2018) Difference between persistent aneurysm, regressed aneurysm, and coronary dilation in Kawasaki Disease: an optical coherence tomography study. Can J Cardiol 34(9):1120–1128. https://doi.org/10.1016/j.cjca.2018.05.021
8. Soriano F, Veas N, Nava S, Piccinelli E, Pedrotti P, Oreglia J, Vignati G, Winter J, Ammirati E, Burns JC, Gordon JB (2021) Late-sequalae of Kawasaki disease characterized by optical coherence tomography. J Cardiovasc Med (Hagerstown) 22(7):597–599. https://doi.org/10.2459/JCM.0000000000001083
9. Kakimoto N, Suzuki H, Kubo T, Suenaga T, Takeuchi T, Shibuta S, Ino Y, Akasaka T, Yoshikawa N (2014) Evaluation of coronary arterial lesions due to Kawasaki disease using optical coherence tomography. Can J Cardiol 30(8):956.e7–9. https://doi.org/10.1016/j.cjca.2014.04.028
10. Ronneberger O, Fischer P, Brox T (2015) U-net: convolutional networks for biomedical image segmentation. In: MICCAI, Springer, pp 234–241
11. Glorot X, Bengio Y (2010) Understanding the difficulty of training deep feedforward neural networks. In: AISTATS, pp 249–256
12. D. P. Kingma, J. Ba, Adam: a method for stochastic optimization, CoRR abs/1412.6980
13. Zhang TY, Suen CY (1984) A fast parallel algorithm for thinning digital patterns. Commun ACM 27(3):236–239
14. Cao TT, Tang K, Mohamed A, Tan TS (2010) Parallel Banding Algorithm to compute exact distance transform with the GPU. In: Proceedings of the 2010 ACM SIGGRAPH symposium on interactive 3D graphics and games, 19–21 February, 2010, Washington DC
15. Hawick K, Leist A, Playne D (2010) Parallel graph component labelling with GPUs and CUDA. Parallel Comput 36(12):655–678
16. Yamakawa R, Ishii M, Sugimura T et al (1998) Coronary endothelial dysfunction after Kawasaki disease: evaluation by intracoronary injection of acetylcholine. J Am Coll Cardiol 31(5):1074–1080. https://doi.org/10.1016/S0735-1097(98)00033-3
17. Suzuki A, Yamagishi M, Kimura K et al (1996) Functional behavior and morphology of the coronary artery wall in patients with Kawasaki disease assessed by intravascular ultrasound. J Am Coll Cardiol 27(2):291–296. https://doi.org/10.1016/0735-1097(95)00447-5
18. Maroules CD, Khera A, Ayers C et al (2014) Cardiovascular outcome associations among cardiovascular megnetic resonance measures of arterial stiffness: the Dallas heart study. J Cardiovasc Magn Reson 16:33
19. Sharif S, Visseren FLJ, Spiering W et al (2019) Arterial stiffness as a risk factor for cardiovascular events and all-causemortality in people with Type 2 diabetes. Diabetes Med 36(9):1125–1132
20. De Bruyne D, Pijls NH, Kalesan B et al (2012) Fractional flow reserve-guided PCI versus medical therapy in stable coronary disease. N Engl J Med 367:991–1001
21. Tonino PA, De Bruyne B, Pijls NH et al (2009) Fractional flow reserve versus angiography for guiding percutaneous coronary intervention. N Engl J Med 360:213–224
22. Fearon WF, Achenbach S, Engstrom T et al (2019) Accuracy of fractional flow reserve derived from coronary angiography. Circulation 139(4):477–484
23. Rajani R, Modi B, Ntalas I, Curzen N (2017) Non-invasive fractional flow reserve using computed tomographic angiography: where are we now and where are we going? Heart 103(15):1216–1222. https://doi.org/10.1136/heartjnl-2016-311029